Estimation of space heating CO 2 emissions based only on CO 2 fluxes observations

Marine Goret, Valéry Masson, Marie-Pierre Moine, William Maurel, Dominique Legain, Grégoire Pigeon

Estimation of space heating CO_2 emissions based only on CO_2 fluxes observations

Marine Goret[a]*, Valéry Masson[a], Marie-Pierre Moine[b], William Maurel[a], Dominique Legain[a] and Grégoire Pigeon[a]

January 17, 2025

Corresponding author : marine.goret@meteo.fr
[a] CNRM, Université de Toulouse, Météo-France, CNRS, Toulouse, France
[b] CECI, Université de Toulouse, CERFACS/CNRS, Toulouse, France

Abstract

Heating buildings is a significant contributor to CO_2 emissions in cities located at mid- and high-latitudes. This study aims to enhance our understanding of the average daily cycle and interseasonal variability of CO_2 emissions from space heating. To achieve this goal, we have developed a methodology solely relying on observations to identify the contribution of space heating to CO_2 fluxes measured in the urban inertial sublayer. This method offers two main advantages. Firstly, it allows for the estimation of space heating contribution with high frequency, facilitating the analysis of its daily cycle. Secondly, our estimation is independent of other methods that do not rely on observations, such as modeling or fuel-consumption based approaches.

Our methodology was developed using original CO_2 flux data measured at rooftop level. Utilizing such data raises theoretical questions. However, the results demonstrate that with adapted processes (non-rotation of data and the exclusion of data with excessively high absolute vertical speeds), the measurements are entirely valid. Our estimation is consistent with estimations made using established methods, such as numerical modeling with the urban canopy model TEB, Heating Degree Days, and gas consumption methods.

1 Introduction

Cities are substantial contributors to anthropogenic CO_2 emissions [Seto et al., 2014]. Consequently, reducing these emissions is imperative within the context of global warming. Assessing CO_2 emissions from cities is crucial for identifying optimal strategies to mitigate emissions and for monitoring their evolution over time.

The most direct method for measuring CO_2 fluxes at the neighborhood scale is using the eddy-covariance method. Over the past two decades, there has been a rapid increase in the number of papers addressing CO_2 eddy covariance measurements in urban environments. This method, initially employed in rural settings, has demonstrated its validity in urban areas [Grimmond et al., 2002; Nemitz et al., 2002; Soegaard and Møller-Jensen, 2003; Grimmond et al., 2004; Moriwaki and Kanda, 2004; Vogt et al., 2006; Järvi et al., 2009a; Kordowski and Kuttler, 2010; Velasco and Roth, 2010; Crawford et al., 2011; Gioli et al., 2012; Järvi et al., 2012; Liu et al., 2012; Nordbo et al., 2012; Velasco et al., 2013, 2014; Crawford et al., 2015; Font et al., 2015; Weissert et al., 2016; Roth et al., 2017; Kleingeld et al., 2018; Björkegren and Grimmond, 2018; Stagakis et al., 2019; Lipson et al., 2022; Park et al., 2022]. Measurements are conducted in the inertial sublayer to capture the total CO_2 flux with high temporal resolution (approximately every 30 minutes). However, the specific contributions of different sources (such as road traffic, space heating, vegetation, human respiration, and factories) to the total flux remain unclear.

Several studies have attempted to tackle the challenge of attributing the contribution of each source. The most commonly employed method involves integrating exogenous data with CO_2 flux measurements and attributing sources through linear regressions. For instance, Nemitz et al. [2002]; Gioli et al. [2012] assigned traffic contributions using traffic counts, while Soegaard and Møller-Jensen [2003] linked space heating to heating degree days. The temporal resolution of attribution methods relies on the temporal resolution of the exogenous data utilized. Traffic data is typically available hourly, whereas space heating data is often limited to daily frequency regardless of the nature of the exogenous data (inventory, degree day method).

Sometimes, the approach involves leveraging wind direction to isolate the most pertinent measurements for each contributor. For instance, to assess traffic contribution, periods with wind originating from sectors with major roads are selected [Järvi et al., 2009b; Crawford and Christen, 2015]. Nonetheless, this method has the drawback of significantly reducing data availability, as only measurements with the appropriate wind direction are considered.

Few authors propose novel methods to address the issue of separating CO_2 fluxes. For example, radiocarbon isotope measurements can differentiate between anthropogenic and biogenic sources, but the temporal resolution is relatively low (few-hour time periods over a week) [Weissert et al., 2016]. Recently, Nicolini et al. [2022] utilized the COVID-19 lockdown period and the ensuing changes in congestion levels to underscore the importance of traffic in residential areas.

This study introduces a novel method relying solely on observations to estimate the contribution of space heating to the total CO_2 flux. This estimation is facilitated by simultaneously observing fluxes at two vertical levels: rooftop level and mast level (the mast is installed on the roof and takes measurements in the inertial sub-layer). The contribution of space heating is assessed by subtracting CO_2 fluxes at rooftop level, which encompass all contributors except space heating, from CO_2 fluxes at mast level, which encompass all contributors. Utilizing only CO_2 flux observations offers the primary advantage of leveraging their high temporal frequency of 30 minutes to estimate CO_2 emissions from space heating at the same frequency. Consequently, we can determine the mean seasonal daily cycles of CO_2 fluxes attributed to space heating. This estimation facilitates the identification of peak periods of CO_2 emissions from space heating throughout the day. Furthermore, it can be utilized to assess and enhance the modeling of CO_2 emissions from space heating with high temporal resolution (ranging from one to a few hours).

Section 2 outlines the datasets utilized in this study, followed by Section 3, which details the methods employed for processing rooftop CO_2 fluxes and estimating CO_2 fluxes attributable to space heating. In Section 4, we compare our estimation of CO_2 emissions from space heating with other methodologies to evaluate its accuracy. Additionally, we examine the daily and seasonal variations in the contribution of space heating. Finally, Section 5 provides a discussion of the results and their implications for future research endeavors.

2 Data

2.1 The CAPITOUL campaign

The CAPITOUL campaign (Canopy and Aerosol Particle Interactions in the Toulouse Urban Layer) was conducted in Toulouse, France, spanning from February 2004 to February 2005 [Masson et al., 2008; Lipson et al., 2022]. Toulouse is situated in the southwest of France, characterized by a temperate climate influenced by both the Atlantic Ocean and the Mediterranean Sea.

The observations utilized in this paper were gathered at the Capitole site, situated in the heart of Toulouse. The neighborhood falls under the Local Climate Zone 2 classification [Stewart and Oke, 2012]. It primarily comprises 4-5 storey brick buildings with very little vegetation.

In the vicinity of the instrumented building (referred to as Monoprix), CO_2 emissions primarily stem from road traffic and nearby buildings [Goret et al., 2019]. Given that a significant portion of the building's contribution comes from space heating, CO_2 fluxes exhibit considerable interseasonal variability, largely influenced by outdoor temperature: fluxes peak in winter (DJF) and are lowest in summer (JJA).

2.2 Observed CO_2 fluxes

2.2.1 Observed CO_2 fluxes at the mast's pinnacle

During the CAPITOUL campaign, a pneumatic mast was installed on the roof of the Monoprix building (refer to Figure 1 for an illustration of the setup). At the mast's pinnacle, throughout the campaign duration (February 2004 - February 2005), an open-path LICOR-7500 measured CO_2 concentration at 20 Hz, while a GILL sonic anemometer recorded wind speed at 50 Hz.

For safety protocols, the mast is retracted during forecasts of strong wind events. When the mast is fully extended, the instruments are positioned at 48.05 m above ground level and 27.5 m above the rooftop level. CO_2 fluxes were computed using the classic eddy-covariance method. The measurements at the mast represent approximately a circle with a radius of 500 metres, centred on the mast (see Figure 2). The footprint analysis was performed using the Flux Footprint Predictions (FFP) model, as described by Kljun et al. [2015] Further details regarding data treatment, quality, and representativeness can be found in Goret et al. [2019].

2.2.2 Observed CO_2 fluxes at roof level

Additional measurements were conducted at roof level utilizing two booms (refer to Figure 3): one positioned over each adjacent street of the Monoprix building, namely Rue de la Pomme and Rue d'Alsace-Lorraine [Masson et al., 2008]. The length of each boom corresponds to one third of the width of the streets. At the terminus of each boom, a YOUNG sonic anemometer and a LICOR-7500 open-path device were installed. They recorded wind speed and CO_2 concentration, respectively, at a frequency of 10 Hz. These measurements are available from June 15th, 2004, to February 28th, 2005.

Data from the gas analyzers (CO_2 concentration) and the anemometers (wind speed and direction) need to undergo filtering and correction before they can be utilized for CO_2 flux calculations. Isolated and non-isolated peaks are eliminated. A value is considered an isolated peak if its absolute deviation from the average of the preceding and succeeding values exceeds 4 m s^{-1} (at 10 Hz) for wind speed and 55 ppm (at 10 Hz) for CO_2 concentration. Non-isolated peaks are characterized by a deviation from the moving mean exceeding six moving standard deviations for wind speed and seven moving standard deviations for CO_2 concentration. Moving averages and standard deviations are calculated over time intervals of 300 s for wind speed and 100 s for CO_2 concentration. Data filtering also encompasses the removal of rain events, identified based on low signal strength received by the LICOR.

CO_2 fluxes are computed using the eddy-covariance method for 30-minute intervals. Several standard corrections are applied, including the Webb correction [Webb et al., 1980]. The time lag between the gas analyzer and the anemometer is adjusted by identifying the maximum correlation between the wind speed and CO_2 concentration time series. Additionally, a high-pass filter with a cut-off frequency of 0.0008 Hz (approximately 1/(20 min)) is employed.

Furthermore, the turbulence stationarity is assessed using the flag proposed by Foken et al. [2004]: the CO_2 fluxes for a 30-minute period are compared with the average of CO_2 fluxes calculated for 5-minute sub-periods. If the flag exceeds five, indicating insufficient stationarity and reflecting data of low quality unsuitable for statistical analysis, the observations are deemed invalid. Moreover, data from July were discarded due to suspicious values.

Following these preprocessing steps, the data availability of CO_2 fluxes is excellent for all seasons with a minimum of 67% availability for each season and for both streets.

2.3 Numerically modelled CO_2 fluxes

A modeling of CO_2 fluxes using the urban canopy model TEB was conducted at the Monoprix site by Goret et al. [2019]. The modeled fluxes, with a 30-minute output time step, showed good agreement with those measured at mast level for the same time intervals. At each time step, the TEB model provides the contribution of the CO_2 flux related to various sources (such as road traffic, buildings, human respiration, and vegetation), along with the total CO_2 flux. In the model, a significant portion of the building contribution is attributed to space heating. Consequently, in this context, the modeled space heating contribution is equated with the modeled building contribution. For this article, we utilize the flux obtained with the reference configuration of the model (referred to as REF in Goret et al. [2019]), which has been demonstrated to yield modeled CO_2 fluxes closest to the observed ones. Estimates of CO_2 emissions from space heating are calculated by TEB in two steps. First, the model estimates the heating energy demand based on the outdoor temperature and building architecture. It then converts this energy into CO_2 emissions using emission factors. This model has been evaluated in several papers: see Pigeon et al. [2014]; Bueno et al. [2012] for the heating energy demand and Goret et al. [2019] for the CO_2 emissions from space heating.

2.4 Statistical estimation of CO_2 fluxes due to space heating

In addition to the observed and numerically modeled fluxes, we also estimated CO_2 fluxes using two other methods: Heating Degree Days and inventory of gas consumption. These methods provide estimates of the heating contribution on a daily time scale.

2.4.1 Heating Degree Days

The HDD method is commonly employed to attribute CO_2 fluxes [Kleingeld et al., 2018; Lietzke et al., 2015; Christen et al., 2011].

Heating Degree Days (HDD) are calculated using the following equation:

$$HDD = max(\mathrm{Thr}_{HEAT} - T_{mean}, 0).$$

Here, HDD represents the Heating Degree Days of the day. T_{mean} denotes the mean temperature of the day, calculated by averaging the minimum and maximum temperatures. Thr_{HEAT} is the threshold temperature below which heating is activated. Following Soegaard and Møller-Jensen [2003], we set it equal to 15.5 °C. Once the HDD value is obtained, the corresponding CO_2 flux is estimated using a linear regression between HDD and the CO_2 flux measured at the mast's pinnacle.

2.4.2 Gas consumption

Gas inventory serves as a reference for evaluating the CO_2 budget of cities or countries. The IPCC has produced a methodological guide for constructing national inventories [Eggleston et al., 2006], and the method is certified by an international standard (ISO 14064-1).

Gas consumption data were collected for the urban area of Toulouse. Due to the interconnected nature of gas supply points, it was not possible to obtain data at a finer spatial scale.

Gas is utilized for various activities such as space heating, cooking, and warming water... It is assumed that the amount of gas used for activities other than space heating remains constant throughout the year, except during summer holidays. During this period, there is a decrease in gas consumption due to a large number of people leaving the Toulouse area for holidays. To estimate the daily quantity of gas used for purposes other than heating, the gas consumption of days with a 0 HDD value was averaged. Data for July and August were excluded to avoid bias resulting from the decrease in gas consumption during the summer.

Similar to the HDD-based estimation, CO_2 fluxes resulting from gas consumption for heating purposes are estimated using linear regression with the CO_2 fluxes measured at the mast's pinnacle.

3 Method

3.1 Specific processing of rooftop level CO_2 fluxes

Very few papers address eddy-covariance CO_2 fluxes at roof level in an urban environment. We found only one paper that does: Lietzke and Vogt [2013]. They measure CO_2 fluxes over one year in an urban environment in Basel at two levels: one measurement point is at roof level, in the middle of the canyon, and the other one is in the inertial sublayer, at 19 meters above a 20-meter high building. Results show a strong dependence of CO_2 fluxes at roof level on traffic. Fluxes above roof level are also correlated with traffic but only for the east wind direction.

Measuring CO_2 fluxes at rooftop level is innovative. However, the methodology to calculate CO_2 fluxes in this environment is not yet well established. We propose a new process to account for the specific measurement conditions present at rooftop level.

Contrary to the usual procedure, and in agreement with Lietzke and Vogt [2013], we do not perform any rotation of the data. Data rotation involves assuming that the mean airflow is parallel to the ground to correct for the lack of horizontality of the anemometer. However, at rooftop level, the proximity of buildings disturbs the airflow, and it is not parallel to the ground. Applying a 2D rotation would often result in rotation angles exceeding 30°. The lack of horizontality of the anemometer is very likely to be only a few degrees. Therefore, assuming that the anemometer is horizontal is a weaker assumption than assuming that the average airflow is parallel to the ground.

A preliminary analysis of the data reveals that negative CO_2 fluxes are frequently recorded. Given the minimal vegetation in the immediate vicinity of the booms, these flux values are implausible, especially in winter. These negative fluxes likely reflect incorrect measurement conditions.

Two parameters can characterize incorrect measurement conditions: the friction velocity and the absolute vertical wind speed. A low friction velocity indicates low turbulence, which may not be sufficient for eddy-covariance measurements. Additionally, the eddy-covariance theory is based on the assumption of zero mean vertical wind. Therefore, excessively high absolute vertical wind speeds could lead to incorrect measurements. Such high values are particularly likely to occur with measurements at roof level, as the airflow is disturbed by nearby buildings.

The data is filtered based on the friction velocity and the absolute mean vertical wind speed. Deciles of these two parameters are determined for each measuring point (Rue de la Pomme and Rue d'Alsace-Lorraine) and then used to form one hundred classes (ten classes for wind speed multiplied by ten classes for friction velocity) in which 30-minute CO_2 flux measurements are divided. For each class, the percentage of negative values of CO_2 fluxes is calculated (Figure 4). This quantity is then used to establish the thresholds of friction velocity and vertical speed which characterize incorrect measurement conditions.

There is no discernible correlation between friction velocity (u*) and the percentage of negative flux values. In some studies in the countriside, u* is used to remove data when turbulence levels are insufficient leading to a decoupling between atmospheric layers near the ground and at the measurement level. Such decoupling is unlikely

to occur in dense urban environment such as the center of Toulouse, where convective turbulent fluxes remain positive most of the time, even at night and the boundary layer remain neutral or slightly positive which guarantee the coupling. Therefore, this parameter should not be used to filter CO_2 flux observations.

In contrast, the absolute vertical wind speed has a significant effect: as it increases, the percentage of negative fluxes also increases. Consequently, a threshold for the maximum admissible absolute vertical wind speed ($|w|$) should be established. The threshold choice involves a trade-off between the number of deleted values, which should be minimized, and the number of remaining negative values, which should be reduced as much as possible. Figure 5 illustrates that a change in the ratio between the number of deleted values and the number of remaining negative values occurs around the threshold value of 0.2 m s^{-1}. By filtering out values with an absolute mean vertical wind speed of 0.2 m s^{-1} or greater, 35% of the data is removed, and the percentage of negative flows is reduced by half (from 10% to 5%).

To evaluate our filtering method, we assess its impact on the mean seasonal daily cycle of CO_2 fluxes (cf. Figure 6). As anticipated, CO_2 fluxes demonstrate an increase across all seasons. Of particular note is the pronounced increase observed in DJF, with the first quartile values after filtering exhibiting a rise of up to 25 micro mol m^{-2} s^{-1} in comparison to the original dataset. Filtering leads to a convergence of the daily cycles of the DJF CO_2 fluxes with the daily cycles of other seasons (both on average and for the different quartiles). This convergence is reasonable because the booms measure fluxes over the urban canyon, and the latter are not expected to show high seasonality (there is very little vegetation in the canyon, and CO_2 emissions from space heating are emitted above the measurement level). The shape of the daily cycles in the different seasons is also reasonable: the fluxes follow the rhythm of anthropogenic activity and more precisely the traffic density (traffic is the main CO_2 emitter in the canyon). There are low emissions at night and higher emissions during the day, with a first peak around 9 UTC and a second higher peak around 16 UTC. Lietzke and Vogt [2013] also reported a strong correlation between CO_2 fluxes at roof level and traffic variability in Basel.

All these results lead to the conclusion that the specific methodology presented here to process CO_2 fluxes is robust enough to handle the specific measurement environment at roof level and to obtain accurate flux observations at that level.

3.2 Estimation of CO_2 emissions due to space heating

Here we propose a method to identify the portion of the CO_2 fluxes attributable to space heating. This method relies solely on the observed CO_2 fluxes. The contribution of space heating is identified by combining the CO_2 flux observations at mast's pinnacle level and roof level.

The following assumptions are made: (1) CO_2 emissions due to heating are all emitted above the rooftop level, (2) the amount of CO_2 released above the rooftop level due to sources other than space heating (domestic warm water production, cooking) is negligible or constant, regardless of the time of day or seasons, (3) fluxes measured at the mast level include all sinks and sources of CO_2 present at the neighborhood scale, (4) fluxes measured at the roof level include all sinks and sources of CO_2 present in the urban canyon, with all contributors that release or uptake CO_2 located below the rooftop level, (5) the variations of CO_2 fluxes measured at the rooftop level over Rue de la Pomme and Rue d'Alsace Lorraine are representative of the ones that could be measured at roof level over all the roads in the neighborhood.

The assertion (1) is based on the observation that smoke vents are typically located on roofs in Toulouse. Hypothesis (2) is a relatively robust assumption; however, it is likely that cooking and domestic water warming are in fact less frequent during the night. Nevertheless, the dataset is not sufficiently large to allow for the incorporation of the daily cycle of these activities in our methodology. Hypotheses (3) and (4) are standard assumptions underlying CO_2 flux measurements. It is highly probable that hypothesis (5) is correct. In the vicinity of the site measurements, there is a scarcity of vegetation, and CO_2 from buildings is rejected over the rooftop level. Therefore, the primary source of CO_2 is vehicular traffic. Traffic count data for six locations within the footprint area, including Rue d'Alsace Lorraine, indicate a homogeneous fluctuation in traffic patterns throughout the neighborhood (see Figure 7). A strong correlation exists between the traffic count at Alsace-Lorraine and the traffic count at the other locations, with a correlated coefficient exceeding 0.96 and a p-value below 5e-14 for all locations.

Given all the above assumptions, we arrive at the following equation:

$$F_{mast} = \alpha * F_{roofs} + F_{HEAT} + \beta \tag{1}$$

where:

- F_{mast} is the CO_2 flux measured at mast level,

Dataset	Other sources	α_{Alsa}	α_{Pom}	β	Number of observations
Alsace	Negligible	0,40	-	0	643
Pomme	Negligible	-	0,53	0	1218
AlsaPom	Negligible	0,22	0,28	0	461
Alsace	Constant	0,26	-	7,7	643
Pomme	Constant	-	0,33	7,7	1218
AlsaPom	Constant	0,14	0,18	7.3	461

Table 1: Values of the coefficients of the linear regressions used to estimate the CO_2 fluxes without space heating at the mast's pinacle. The unit of β is µmol m^{-2} s^{-1}. The number of observations is limited by the need to have observations at roof level and mast level simultaneously.

- F_{roofs} is the CO_2 flux measured above roads, at rooftop level (using booms),
- F_{HEAT} is the CO_2 flux due to space heating of buildings (and emitted above rooftop level),
- α and β are coefficients to be determined.

The coefficient α depends on the road fraction via the dilution phenomenon at the top of the street canyon, and on the relative importance of the fluxes measured at rooftop level compared to the mean CO_2 flux of the neighborhood at the same level: the more important these measured fluxes are, the lower α will be. α and β coefficients are determined experimentally using data collected during the summer season (JJA). At that time of the year, due to the absence of space heating, Equation 1 becomes:

$$F_{mast} = \alpha * F_{roofs} + \beta, \tag{2}$$

The CO_2 fluxes measured at the mast's pinnacle are plotted against the fluxes measured at rooftop level during JJA period (not shown). Subsequently, a linear regression is adjusted using the least squares method. From equation 2 the slope of this line represents the value of α, while the intercept represents the β value.

The CO_2 released above roofs and emitted by sources other than space heating is assumed to be either negligible or constant. These two assumptions are tested separately: β is set at 0 if other sources are assumed to be negligible, and it is non-zero when they are assumed to be constant.

In order to test the robustness of the method (see section 3.3 for more explanations), we constructed three datasets of CO_2 fluxes measured at rooftop level. The first dataset contains fluxes measured above the Rue de la Pomme (Pomme dataset), the second dataset contains fluxes measured above the Rue d'Alsace-Lorraine (Alsace dataset), and the third one is the union of the two previous datasets (AlsaPom dataset). For the third dataset, the multiplication $\alpha * F_{roofs}$ must be considered as a vector/matrix product, and Equation 2 can be rewritten as:

$$F_{mast} = \alpha_{Alsa} * F_{roofs_{Alsa}} + \alpha_{Pom} * F_{roofs_{Pom}} + \beta \tag{3}$$

Once the coefficients α and β have been estimated for the summer season (JJA), the CO_2 flux for all seasons can be split between the flux related to space heating and the flux related to all other contributors:

$$F_{OTH} = \alpha * F_{roofs} + \beta \tag{4}$$

$$F_{HEAT} = F_{mast} - F_{OTH} \ ; \tag{5}$$

where F_{OTH} is the CO_2 flux due to all other contributors than space heating.

3.3 Assessment of the different regression methods to estimate the contribution of space heating to the total CO_2 flux

Six pairs of values for α and β are evaluated using JJA measurements (space heating being turned off during this season), considering the three datasets and the two assumptions on β. The values are summarized in Table 1. These six pairs allow for six different reconstructions of the CO_2 fluxes at mast level from the measured CO_2 fluxes at roof level. The quality of each reconstruction is evaluated by comparing the mean daily cycle of the reconstructed CO_2 fluxes with the mean daily cycle of the observed fluxes at the mast's pinacle (Figure 8).

During the day, all the reconstructions yield similar results, in good agreement with the observations. However, in the evening and at night, the reconstructions can be divided into two groups: those assuming that the CO_2 emitted above rooftop by sources other than space heating is negligible (Negligible group) and those assuming that it is constant (Constant group). In the evening (18 UTC to 23 UTC), the observations align more closely with the estimates of the Constant reconstruction group. At night (23 UTC to 6 UTC), the observations fall between the estimates of each of the two reconstruction groups. Neither hypothesis (Negligible or Constant) allows for an accurate reconstruction of the daily cycle of observed CO_2 fluxes. This demonstrates that neither hypothesis is entirely correct, and in reality, CO_2 emissions above roofs from sources other than space heating follow a daily cycle (the occurrence of cooking activities and water warming both decrease during the late-night and early-morning hours). However, the combination of the estimates obtained for each group enables a more accurate estimation of the cycle: the observed fluxes fall within the range of values from the two reconstruction groups.

In light of the aforementioned observations, we propose a numerical estimate of the uncertainty associated with our disaggregation method. To this end, for each CO_2 flux value reconstructed at the mast level, we calculate the difference between the reconstructed value and the measured value:

$$e_{i,r,h} = r_{i,r,h} - o_{i,r,h} \tag{6}$$

where e is the reconstruction error, r the reconstructed value and o the observed value. The variables i, r and h are used to refer to the i^{th} observation for the regression r and the hour h. The mean error for the regression r and the hour h is given by the following expression, where $N_{r,h}$ denotes the number of values available for a specific regression and hour.

$$\bar{e}_{r,h} = \frac{1}{N_{r,h}} \sum_{i=1}^{N_{r,h}} e_{i,r,h} \tag{7}$$

Then, the uncertainty, which is calculated as twice the standard deviation of the differences between the reconstructed values and the observed values, can be written as follows:

$$U(r,h) = 2 * \sqrt{\frac{1}{N_{r,h}-1} * \sum_{i=1}^{N_{r,h}} (e_{i,r,h} - \bar{e}_{r,h})^2} \tag{8}$$

This uncertainty is graphically represented in Figure 8 with error bar. During the day, when CO_2 fluxes are larger and data availability is smaller, the uncertainty is larger. At night, there is a systematic negative/positive bias for the Negligible/Constant group that can be attributed to the daily cycle of the so-called other sources, which is not accounted for in this study. The larger uncertainty associated with the AlsaPom dataset can be directly attributed to the coarse availability of data for this particular dataset.

The results indicate that the dataset selected has a negligible effect on the reconstructed CO_2 flux values. Rue de la Pomme and Rue d'Alsace-Lorraine CO_2 fluxes are independently measured. Thus, the good agreement of the estimates obtained with these two datasets indicates that a signal is indeed present in the CO_2 fluxes measured at the rooftop level, despite a measurement environment that is at the limit of the theoretical hypotheses of the eddy-covariance method. It validates, a posteriori, the relevance of CO_2 flux measurements by the eddy-covariance method at rooftop level.

4 Results

4.1 Comparison of CO_2 emissions from space heating: observation-based versus traditional methods at a daily scale

In this section, we compare our estimation of CO_2 fluxes attributable to space heating, solely based on observations, with independent methods: numerical modeling with TEB (refer to section 2.3), gas inventory, and Heating Degree Days (refer to section 2.4).

As the two latter methods provide daily results, the comparison between the different methods is conducted on a daily basis.

Observations are available from June 15th, 2004, to February 28th, 2005. The time series of the different methods are compared in Figure 9. The TEB model and HDD estimations show excellent agreement throughout the period. However, the gas estimation method tends to provide slightly higher estimations. This difference may be attributed

to the representativeness of the gas data, which covers the entire Toulouse metropolitan area, differing from the representativeness of the other methods, which focus on the neighborhood of Monoprix. Towards the end of August, a spike is present in the gas-based estimation, which remains unexplained (it could be the result of erroneous gas inventory). It is evident that this spike does not have any meteorological explanation.

Our observation-based estimation generally aligns well with other methods. Instances where there are larger discrepancies typically coincide with days when there is a low percentage of observations available. Consequently, due to these low percentages, daily mean estimations may only be representative of a certain period of the day (for instance, the morning), during which CO_2 fluxes due to space heating can differ significantly from the average over a 24-hour window. The quality of agreement between our method and the others remains consistent regardless of the dataset considered (Alsace, Pomme, and AlsaPom).

On Figure 10 we compare the dependency of the different estimations on the Heating Degree Day (HDD) when we assume that space heating is on (HDD strictly above 0). Data are filtered to retain only days for which observation-based estimation at a 30-minute frequency is available for more than 60% of the time. This filtering aims to avoid biases due to data availability. Futhermore, we only

Similar to the previous figure, we find that HDD and TEB model estimations are very close. The gas method exhibits a stronger values, consistent with the stronger estimation via the gas method found earlier. The observation-based method aligns well with the other methods for both the Negligible and Constant groups. The slope of the linear regression with HDD is found to be highly consistent across all methods. The observed differences are not statistically significant.The lowest estimated value is for gas, for which the 95% confidence interval ranges from 2.28 to 2.99. The highest values are for observations with the Constant hypothesis, with a confidence interval ranging from 2.0 to 3.69. All confidence intervals are overlapping.

These results provide confidence in our method for estimating CO_2 fluxes due to space heating at the daily time scale. In the next section, we delve into its capability to capture the daily cycle of CO_2 space heating releases.

4.2 Daily CO_2 flux cycle: space heating contribution vs. other sources

As mentioned previously, our objective is to partition the total CO_2 flux measured at the mast's pinnacle into the contributions from space heating and other sources. This partitioning can be achieved for the three seasons during which CO_2 fluxes have been concurrently measured at rooftop and mast levels (DJF, JJA, and SON), using equations 4 and 5.

The values of α and β are obtained from the six pairs of values identified in Section 3.3. Consequently, this results in six different evaluations for both parts of the CO_2 flux. For each pair, the mean, first quartile, and third quartile of F_{HEAT} and F_{OTH} are calculated with a 30-minute time step. The averages of these statistics are then computed by group (Negligible and Constant) to obtain values at group scale. Figure 11 compares the daily cycles obtained through this method with the results of the TEB model (see Section 2.3).

The estimated daily cycles of F_{OTH} across the three seasons exhibit remarkable similarity: JJA and SON cycles are correlated at 97% and JJA and DJF cycles at 92%. This consistency is expected, as the removal of space heating effects results in minimal interseasonal variability in CO_2 fluxes around the measurement mast. The area's sparse vegetation and relatively stable road traffic explain this uniformity from one season to another.

The differences between the two hypothesis groups in DJF and SON are consistent with those observed in JJA: minimal distinctions during the day, with the Constant group showing higher estimates at night compared to the Negligible group. Throughout the day, the Negligible group exhibits an interquartile range that encompasses that of the Constant group.

When combining estimates from both observation groups following the method described in Section 3.3, the TEB model aligns closely with observations. During the night (23 UTC–6 UTC), the model's results fall within the range of estimates from each group. Throughout the day, the model and the estimates exhibit close agreement, with the model closely tracking the estimates obtained for the Constant group in the evening (18 UTC–23 UTC). In the period between 9 and 18 UTC, the TEB model estimation of space heating is significantly lower than our estimation, falling outside the error bars. This suggests that the TEB model may underestimate space heating. This could be due to the model's representation of building isolation, which may not fully account for potential thermal bridges and the numerous door openings of shops, which can lead to heat loss.

On the one hand, the agreement between the estimations and the model in JJA was expected, as in summer, F_{OTH} represents the entirety of the CO_2 flux (no space heating at that period), and as shown in Section 3.3,

observations-based estimations align well with the observations at mast level. Additionally, Goret et al. [2019] highlights the agreement between observations at mast level and the model.

On the other hand, the agreement in SON and DJF validates the possibility of isolating the space heating contribution to the total CO_2 flux at high frequency, thanks to the combination of CO_2 flux observations at roof level and at the mast's pinacle.

This result gives us great confidence in the observation-based estimates of daily cycle emissions due to space heating. Figure 11 shows that CO_2 fluxes are higher in DJF than in SON, and they are almost zero in JJA, which is consistent with expectations. We observe the same model/estimation agreement as previously: the model falls between the estimations made with the two-hypothesis groups at night and follows the estimation of the Constant group in the evening. During the day, the model values are at the lower boundary of the estimates but still remain within the interquartile range. As the model and the observation-based estimates are two independent methods, their mutual agreement is an additional argument for the suitability of both methods. The general daily pattern of CO_2 emissions from space heating is also confirmed: low emissions at night and higher emissions during the day.

5 Discussion

The measurement of CO_2 flux above streets, at rooftop level, does not adhere to all the theoretical assumptions of the flux measurement using the eddy covariance method. In particular, the airflow is not strictly parallel to the surface, and the vertical velocity values may exceed those typically found in the inertial sublayer above. Nevertheless, the application of specific methods such as non-rotation of data and the exclusion of data with excessively high absolute vertical speeds enables the acquisition of usable data with a valid physical signal.

We have developed a new methodology to estimate the CO_2 flux attributable to space heating based solely on observations. This method has been evaluated at both daily and hourly resolutions against previously validated techniques. The results demonstrate a good agreement with these methods, indicating promising prospects for future studies. While the uncertainty associated with this estimation remains relatively high, the general shape of the mean daily cycle of CO_2 fluxes due to space heating is discernible. This finding is particularly noteworthy considering that data related to space heating, such as fuel consumption, are typically available at temporal resolutions no higher than one day. The uncertainty in the estimate could potentially be reduced in future studies by utilizing longer time series of CO_2 flux observations.

Nevertheless, our disaggregating method has already demonstrated its potential, as it allows for the identification of space heating as the contributing factor responsible for the slight underestimation of CO_2 fluxes by the TEB model during the day. Furthermore, it is evident that among the various versions of the TEB model proposed in Goret et al. [2019], only the REF version is consistent with the observed CO_2 flux associated with space heating. This corroborates the hypothesis regarding the space heating setpoint which postulates that individuals utilize a two-degree lower setpoint at night. This conclusion can be reached as our method offers several advantages in comparison to others (Heating Degree Days, gaz consumption...). It is based solely on CO_2 flux observations, eliminating the need for exogenous data, which allows for an estimation that is entirely independent of the modeled one. Additionally, it has a high temporal resolution (30 minutes) and a relatively high spatial resolution, that of a neighborhood. In the future, the method presented here may assist in the evaluation of other numerical modeling and facilitate the monitoring of CO_2 emissions from space heating.

Using longer time series would offer two main advantages: reducing uncertainty by incorporating more data and allowing for the application of different linear regressions for different times of the day. In the current study, we made two distinct assumptions regarding the daily cycle of CO_2 emissions above rooftop level that could not be attributed to space heating: either it remains constant and nonzero, or it is assumed to be zero. It has been demonstrated that neither of these assumptions is entirely accurate. However, by combining both assumptions, upper and lower bounds can be derived. Employing different linear regressions would enable us to evaluate the assumption that CO_2 emitted above rooftop level by sources other than space heating follows a daily cycle. Consequently, we will likely not only obtain bounds for the daily cycle of CO_2 emissions from space heating but also a better fit of this value, leading to a reduction in the uncertainty of its estimation

In conclusion, we have demonstrated that both observation-based and model-based estimations of CO_2 emissions from space heating yield compatible results. These estimations could serve as reference datasets for model calibration and evaluation. Having models capable of accurately representing CO_2 fluxes is crucial in the context of climate change. Such models are valuable for assessing the effectiveness of CO_2 reduction policies and understanding the relationship between global warming and CO_2 emissions from space heating.

6 Declaration of Generative AI and AI-assisted technologies in the writing process

During the preparation of this work the authors used ChatGPT3.5 in order to to improve readability and language. After using this tool/service, the authors reviewed and edited the content as needed and take full responsibility for the content of the publication.

7 CRediT authorship contribution statement

Marine Goret: Writing – original draft, Visualization, Software, Methodology, Conceptualization. Valéry Masson: Writing – review & editing, Supervision, Methodology, Conceptualization. Marie-Pierre Moine: Writing – review & editing, Conceptualization. William Maurel: Resources, Data curation. Dominique Legain: Resources. Grégoire Pigeon: Resources.

8 Declaration of competing interest

The authors declare that they have no known competing financial interests or personal relationships that could have appeared to influence the work reported in this paper.

9 Data availability

Data will be made available on request.

References

Björkegren, A. and Grimmond, C. (2018). Net carbon dioxide emissions from central London. *Urban Climate*, 23:131–158.

Bueno, B., Pigeon, G., Norford, L. K., Zibouche, K., and Marchadier, C. (2012). Development and evaluation of a building energy model integrated in the TEB scheme. *Geoscientific Model Development*, 5(2):433–448.

Christen, A., Coops, N. C., Crawford, B. R., Kellett, R., Liss, K. N., Olchovski, I., Tooke, T. R., van der Laan, M., and Voogt, J. A. (2011). Validation of modeled carbon-dioxide emissions from an urban neighborhood with direct eddy-covariance measurements. *Atmospheric Environment*, 45(33):6057–6069.

Crawford, B. and Christen, A. (2015). Spatial source attribution of measured urban eddy covariance CO2 fluxes. *Theoretical and Applied Climatology*, 119(3-4):733–755.

Crawford, B., Christen, A., and McKendry, I. (2015). Diurnal Course of Carbon Dioxide Mixing Ratios in the Urban Boundary Layer in Response to Surface Emissions. *Journal of Applied Meteorology and Climatology*, 55(3):507–529.

Crawford, B., Grimmond, C. S. B., and Christen, A. (2011). Five years of carbon dioxide fluxes measurements in a highly vegetated suburban area. *Atmospheric Environment*, 45(4):896–905.

Eggleston, H. S., Buendia, L., Miwa, K., Ngara, T., and Tanabe, K. (2006). 2006 IPCC Guidelines for National Greenhouse Gas Inventories. Technical report, IPCC, Japan.

Foken, T., Göockede, M., Mauder, M., Mahrt, L., Amiro, B., and Munger, W. (2004). Post-field data quality control. In *Handbook of micrometeorology*, pages 181–208. Springer.

Font, A., Grimmond, C. S. B., Kotthaus, S., Morguí, J. A., Stockdale, C., O'Connor, E., Priestman, M., and Barratt, B. (2015). Daytime CO2 urban surface fluxes from airborne measurements, eddy-covariance observations and emissions inventory in Greater London. *Environmental Pollution*, 196:98–106.

Gioli, B., Toscano, P., Lugato, E., Matese, A., Miglietta, F., Zaldei, A., and Vaccari, F. P. (2012). Methane and carbon dioxide fluxes and source partitioning in urban areas: The case study of Florence, Italy. *Environmental Pollution*, 164:125–131.

Goret, M., Masson, V., Schoetter, R., and Moine, M.-P. (2019). Inclusion of CO2 flux modelling in an urban canopy layer model and an evaluation over an old European city centre. *Atmospheric Environment: X*, page 100042.

Grimmond, C. S. B., King, T. S., Cropley, F. D., Nowak, D. J., and Souch, C. (2002). Local-scale fluxes of carbon dioxide in urban environments: methodological challenges and results from Chicago. *Environmental Pollution*, 116, Supplement 1:S243–S254.

Grimmond, C. S. B., Salmond, J. A., Oke, T. R., Offerle, B., and Lemonsu, A. (2004). Flux and turbulence measurements at a densely built-up site in Marseille: Heat, mass (water and carbon dioxide), and momentum. *Journal of Geophysical Research: Atmospheres*, 109(D24):D24101.

Järvi, L., Mammarella, I., Eugster, W., Ibrom, A., Siivola, E., Dellwik, E., Keronen, P., Burba, G., and Vesala, T. (2009a). Comparison of net CO2 fluxes measured with open- and closed-path infrared gas analyzers in an urban complex environment. *Boreal Environment Research*, 14:16.

Järvi, L., Nordbo, A., Junninen, H., Riikonen, A., Moilanen, J., Nikinmaa, E., and Vesala, T. (2012). Seasonal and annual variation of carbon dioxide surface fluxes in Helsinki, Finland, in 2006–2010. *Atmos. Chem. Phys.*, 12(18):8475–8489.

Järvi, L., Rannik, \., Mammarella, I., Sogachev, A., Aalto, P. P., Keronen, P., Siivola, E., Kulmala, M., and Vesala, T. (2009b). Annual particle flux observations over a heterogeneous urban area. *Atmospheric Chemistry and Physics*, 9(20):7847–7856.

Kleingeld, E., van Hove, B., Elbers, J., and Jacobs, C. (2018). Carbon dioxide fluxes in the city centre of Arnhem, A middle-sized Dutch city. *Urban Climate*, 24:994–1010.

Kljun, N., Calanca, P., Rotach, M. W., and Schmid, H. P. (2015). A simple two-dimensional parameterisation for Flux Footprint Prediction (FFP). *Geosci. Model Dev.*, 8(11):3695–3713.

Kordowski, K. and Kuttler, W. (2010). Carbon dioxide fluxes over an urban park area. *Atmospheric Environment*, 44(23):2722–2730.

Lietzke, B. and Vogt, R. (2013). Variability of CO2 concentrations and fluxes in and above an urban street canyon. *Atmospheric Environment*, 74:60–72.

Lietzke, B., Vogt, R., Feigenwinter, C., and Parlow, E. (2015). On the controlling factors for the variability of carbon dioxide flux in a heterogeneous urban environment. *International Journal of Climatology*, 35(13):3921–3941.

Lipson, M., Grimmond, S., Best, M., Chow, W. T. L., Christen, A., Chrysoulakis, N., Coutts, A., Crawford, B., Earl, S., Evans, J., Fortuniak, K., Heusinkveld, B. G., Hong, J.-W., Hong, J., Järvi, L., Jo, S., Kim, Y.-H., Kotthaus, S., Lee, K., Masson, V., McFadden, J. P., Michels, O., Pawlak, W., Roth, M., Sugawara, H., Tapper, N., Velasco, E., and Ward, H. C. (2022). Harmonized gap-filled datasets from 20 urban flux tower sites. *Earth System Science Data*, 14(11):5157–5178. Publisher: Copernicus GmbH.

Liu, H. Z., Feng, J. W., Järvi, L., and Vesala, T. (2012). Four-year (2006–2009) eddy covariance measurements of CO2 flux over an urban area in Beijing. *Atmos. Chem. Phys.*, 12(17):7881–7892.

Masson, V., Gomes, L., Pigeon, G., Liousse, C., Pont, V., Lagouarde, J.-P., Voogt, J., Salmond, J., Oke, T. R., Hidalgo, J., Legain, D., Garrouste, O., Lac, C., Connan, O., Briottet, X., Lachérade, S., and Tulet, P. (2008). The Canopy and Aerosol Particles Interactions in TOulouse Urban Layer (CAPITOUL) experiment. *Meteorology and Atmospheric Physics*, 102(3-4):135–157.

Moriwaki, R. and Kanda, M. (2004). Seasonal and Diurnal Fluxes of Radiation, Heat, Water Vapor, and Carbon Dioxide over a Suburban Area. *Journal of Applied Meteorology*, 43(11):1700–1710.

Nemitz, E., Hargreaves, K. J., McDonald, A. G., Dorsey, J. R., and Fowler, D. (2002). Micrometeorological Measurements of the Urban Heat Budget and CO2 Emissions on a City Scale. *Environmental Science & Technology*, 36(14):3139–3146.

Nicolini, G., Antoniella, G., Carotenuto, F., Christen, A., Ciais, P., Feigenwinter, C., Gioli, B., Stagakis, S., Velasco, E., Vogt, R., Ward, H. C., Barlow, J., Chrysoulakis, N., Duce, P., Graus, M., Helfter, C., Heusinkveld, B., Järvi, L., Karl, T., Marras, S., Masson, V., Matthews, B., Meier, F., Nemitz, E., Sabbatini, S., Scherer, D., Schume, H., Sirca, C., Steeneveld, G.-J., Vagnoli, C., Wang, Y., Zaldei, A., Zheng, B., and Papale, D. (2022). Direct observations of CO2 emission reductions due to COVID-19 lockdown across European urban districts. *Science of The Total Environment*, 830:154662.

Nordbo, A., Järvi, L., and Vesala, T. (2012). Revised eddy covariance flux calculation methodologies – effect on urban energy balance. *Tellus B: Chemical and Physical Meteorology*, 64(1):18184.

Park, C., Jeong, S., Park, M.-S., Park, H., Yun, J., Lee, S.-S., and Park, S.-H. (2022). Spatiotemporal variations in urban CO2 flux with land-use types in Seoul. *Carbon Balance and Management*, 17(1):3.

Pigeon, G., Zibouche, K., Bueno, B., Le Bras, J., and Masson, V. (2014). Improving the capabilities of the Town Energy Balance model with up-to-date building energy simulation algorithms: an application to a set of representative buildings in Paris. *Energy and Buildings*, 76(Supplement C):1–14.

Roth, M., Jansson, C., and Velasco, E. (2017). Multi-year energy balance and carbon dioxide fluxes over a residential neighbourhood in a tropical city. *International Journal of Climatology*, 37(5):2679–2698.

Seto, K. C., Dhakal, S., Bigio, A., Blanco, H., Delgado, G., Dewar, D., Huang, L., Inaba, A., Kansal, A., Lwasa, S., McMahon, J., Müller, D., Murakami, J., Nagendra, H., and Ramaswami, A. (2014). *Human Settlements, Infrastructure and Spatial Planning. In: Climate Change 2014: Mitigation of Climate Change. Contribution of Working Group III to the Fifth Assessment Report of the Intergovernmental Panel on Climate Change [Edenhofer, O., R. Pichs-Madruga, Y. Sokona, E. Farahani, S. Kadner, K. Seyboth, A. Adler, I. Baum, S. Brunner, P. Eickemeier, B. Kriemann, J. Savolainen, S. Schlömer, C. von Stechow, T. Zwickel and J.C. Minx (eds.)]*. Cambridge University Press, Cambridge, United Kingdom and New York, NY, USA.

Soegaard, H. and Møller-Jensen, L. (2003). Towards a spatial CO2 budget of a metropolitan region based on textural image classification and flux measurements. *Remote Sensing of Environment*, 87(2-3):283–294.

Stagakis, S., Chrysoulakis, N., Spyridakis, N., Feigenwinter, C., and Vogt, R. (2019). Eddy Covariance measurements and source partitioning of CO2 emissions in an urban environment: Application for Heraklion, Greece. *Atmospheric Environment*, 201:278–292.

Stewart, I. D. and Oke, T. R. (2012). Local Climate Zones for Urban Temperature Studies. *Bulletin of the American Meteorological Society*, 93(12):1879–1900.

Velasco, E., Perrusquia, R., Jiménez, E., Hernández, F., Camacho, P., Rodríguez, S., Retama, A., and Molina, L. T. (2014). Sources and sinks of carbon dioxide in a neighborhood of Mexico City. *Atmospheric Environment*, 97:226–238.

Velasco, E. and Roth, M. (2010). Cities as Net Sources of CO2: Review of Atmospheric CO2 Exchange in Urban Environments Measured by Eddy Covariance Technique: Urban CO2 flux measurements by eddy covariance. *Geography Compass*, 4(9):1238–1259.

Velasco, E., Roth, M., Tan, S. H., Quak, M., Nabarro, S. D. A., and Norford, L. (2013). The role of vegetation in the CO2 flux from a tropical urban neighbourhood. *Atmos. Chem. Phys.*, 13(20):10185–10202.

Vogt, R., Christen, A., Rotach, M. W., Roth, M., and Satyanarayana, A. N. V. (2006). Temporal dynamics of CO2 fluxes and profiles over a Central European city. *Theoretical and Applied Climatology*, 84(1-3):117–126.

Webb, E. K., Pearman, G. I., and Leuning, R. (1980). Correction of flux measurements for density effects due to heat and water vapour transfer. *Quarterly Journal of the Royal Meteorological Society*, 106(447):85–100.

Weissert, L., Salmond, J., Turnbull, J., and Schwendenmann, L. (2016). Temporal variability in the sources and fluxes of CO2 in a residential area in an evergreen subtropical city. *Atmospheric Environment*, 143:164–176.

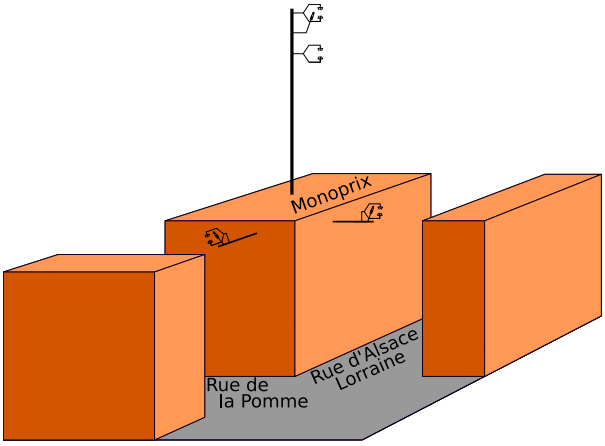

Figure 1: The measurement device used to measure CO_2 fluxes during the CAPITOUL campaign.

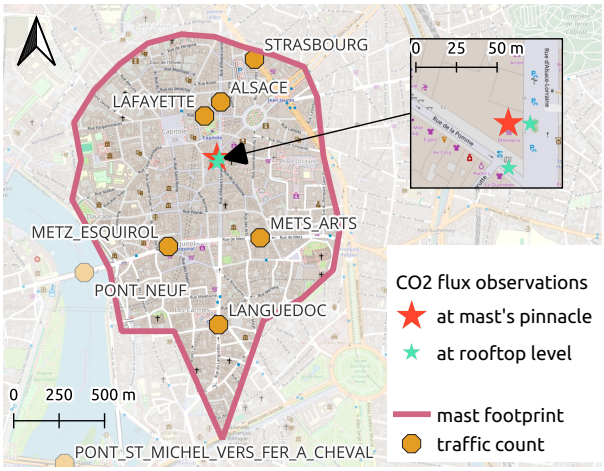

Figure 2: The site environment map depicts the CO_2 flux measurement stations, the footprint for the measurement at the mast's pinacle, and the traffic count stations. The footprint is defined as the minimal area centred on the mast, ensuring that at least 80% of the CO_2 measured at the mast is emitted within the footprint area.

Figure 3: Pictures of the booms employed to measure CO_2 fluxes at rooftop level during the CAPITOUL campaign. Credits : CNRM.

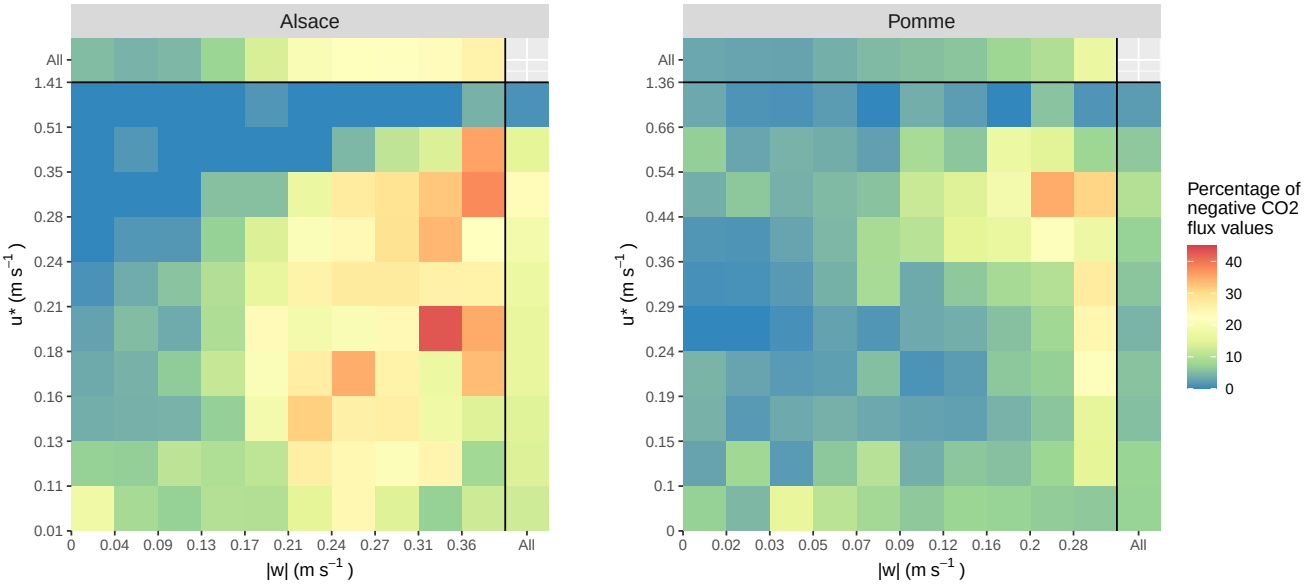

Figure 4: Percentages of negative CO_2 flux values are plotted against the friction velocity (u^*) and the absolute value of the mean vertical wind speed ($|w|$). The class limits correspond to the deciles of the two samples. The results are presented separately for Rue d'Alsace-Lorraine (left panel) and Rue de la Pomme (right panel). The right margins of the figures display the percentages of negative values for the ten classes determined by the deciles of the friction velocity, while the top margins show the percentages for the classes determined by the deciles of the absolute vertical wind speed.

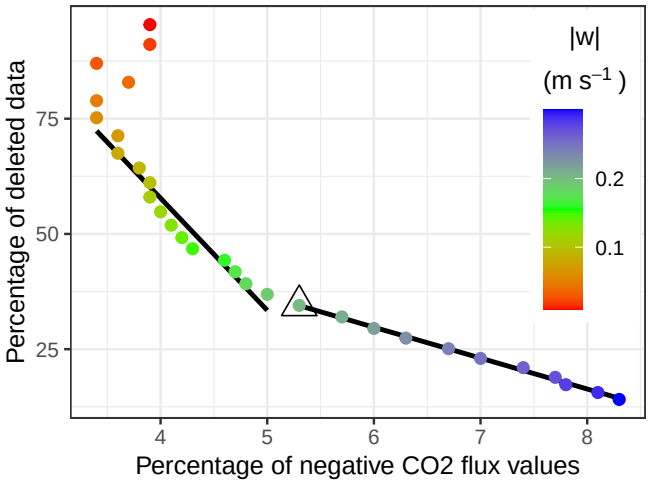

Figure 5: The graph illustrates the number of deleted CO_2 flux values and the number of remaining negative flux values for various thresholds for the maximum absolute vertical wind speed ($|w|$). A black triangle indicates the point corresponding to a threshold of 0.2 m s^{-1}. A steeper slope indicates that more values are removed to eliminate a given amount of negative values. The slope becomes steeper when the threshold is lower than 0.2 m s^{-1}.

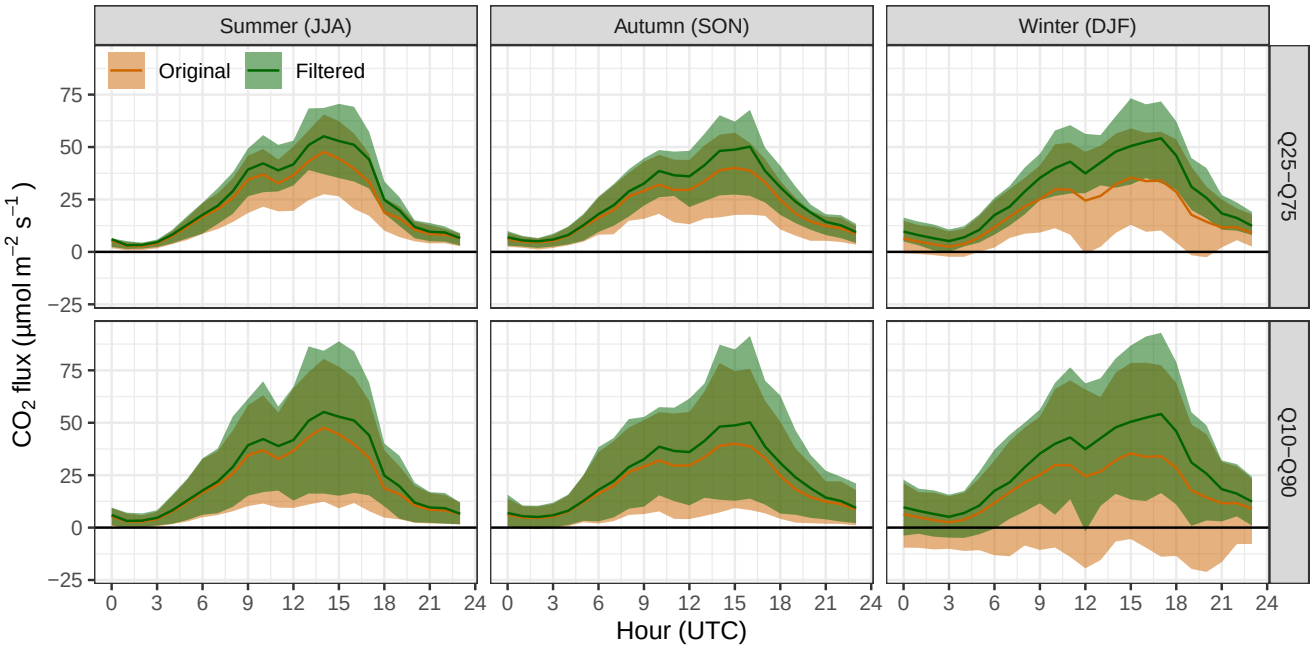

Figure 6: Daily cycles of CO_2 fluxes per season, measured above streets, at rooftop-level, before and after filtering. The coloured ranges indicate the interquartile range (top), and the range between the first and ninth deciles (bottom). The solid lines indicate the mean daily cycles.

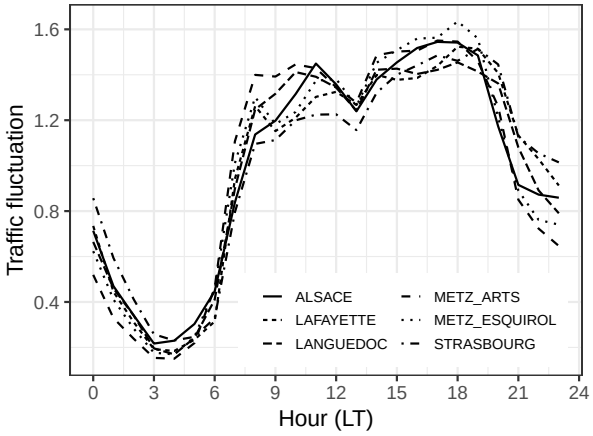

Figure 7: Daily fluctuations in traffic volume at six distinct locations. Refer to Figure 2 for the location of the traffic count stations.

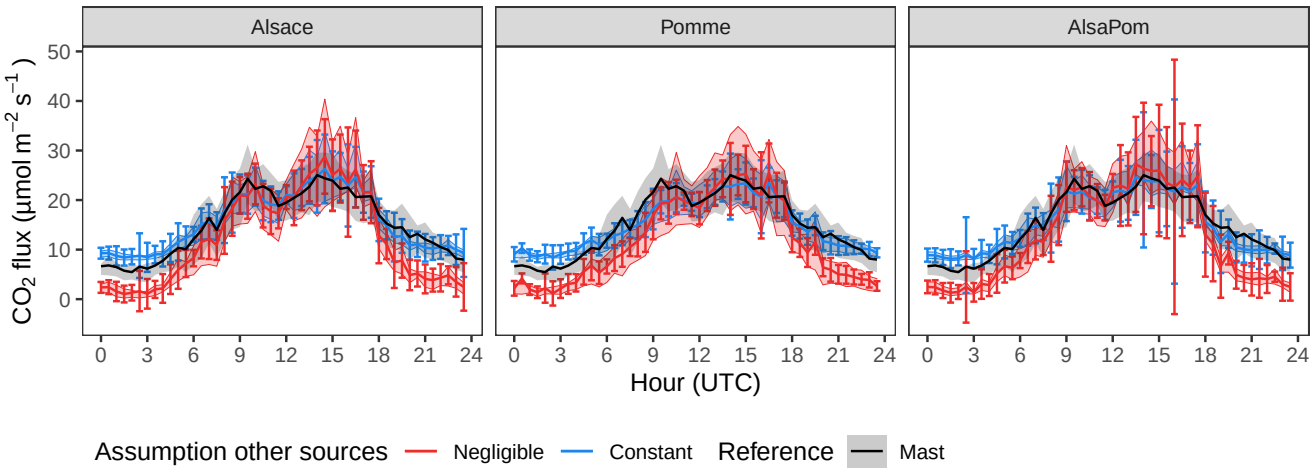

Figure 8: Daily cycles of CO_2 fluxes in JJA, in the center of Toulouse. In black, the cycle observed at mast level. In color, the reconstruction of the cycle at mast's pinacle from the observations of the booms located at rooftop level. The different panels correspond to the different data sets. The coloured areas represent the interquartile range. The error bars indicate the margin of uncertainty associated with the disaggregation method.

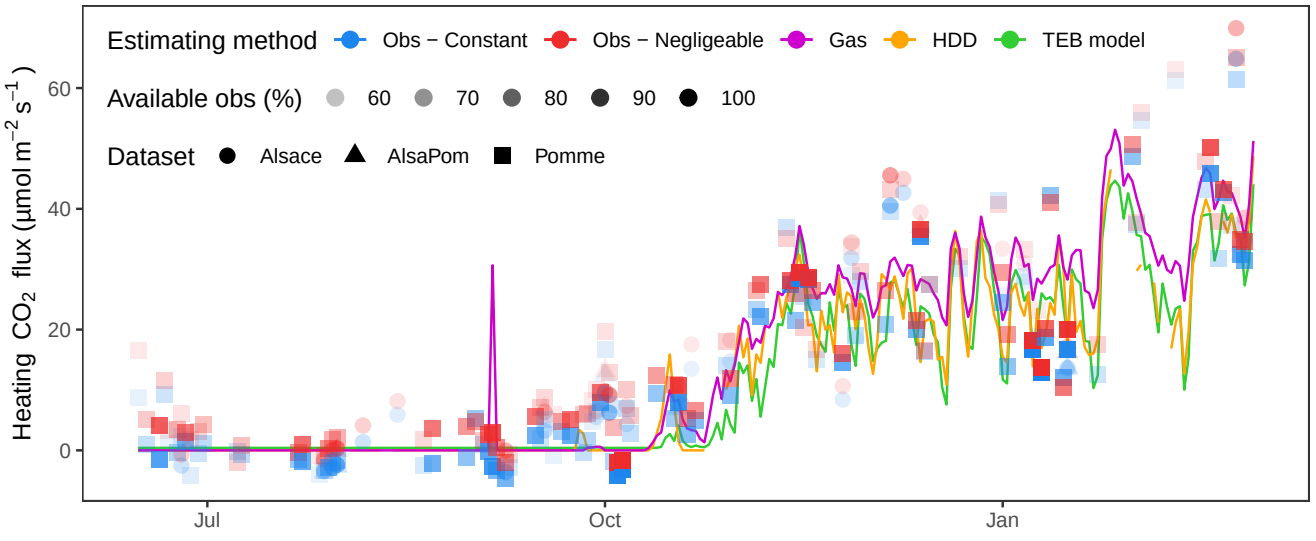

Figure 9: Time series of daily CO_2 fluxes attributed to heating, estimated using various methods: observation-based estimations (Obs - Constant and Obs - Negligible), gas inventory, Heating Degree Day, and numerical modeling. Marker opacity varies based on the percentage of availability of 30-minute observations for each day. Different marker shapes represent the three different datasets.

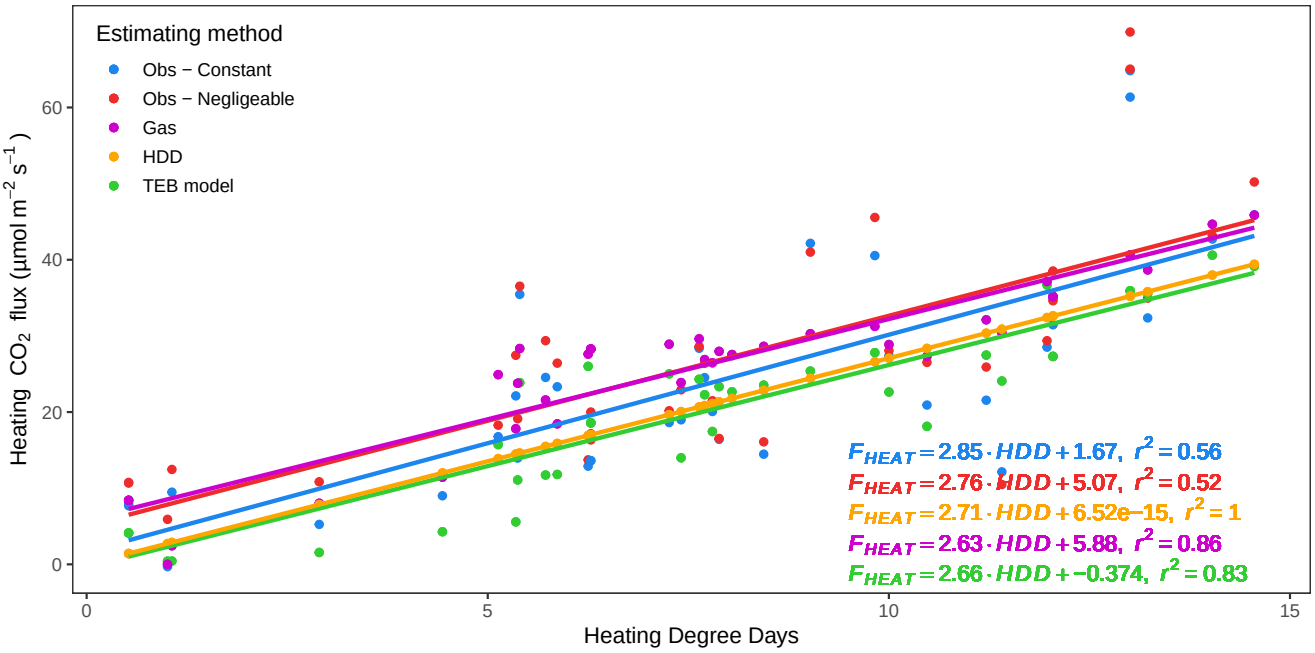

Figure 10: Linear regressions of daily CO_2 fluxes due to space heating with Heating Degree Days for several methods of estimations (see Figure 9 for details). We only keep days for which CO_2 observations-based estimations are available more than 60% of the time, and HDD is strictly above 0.

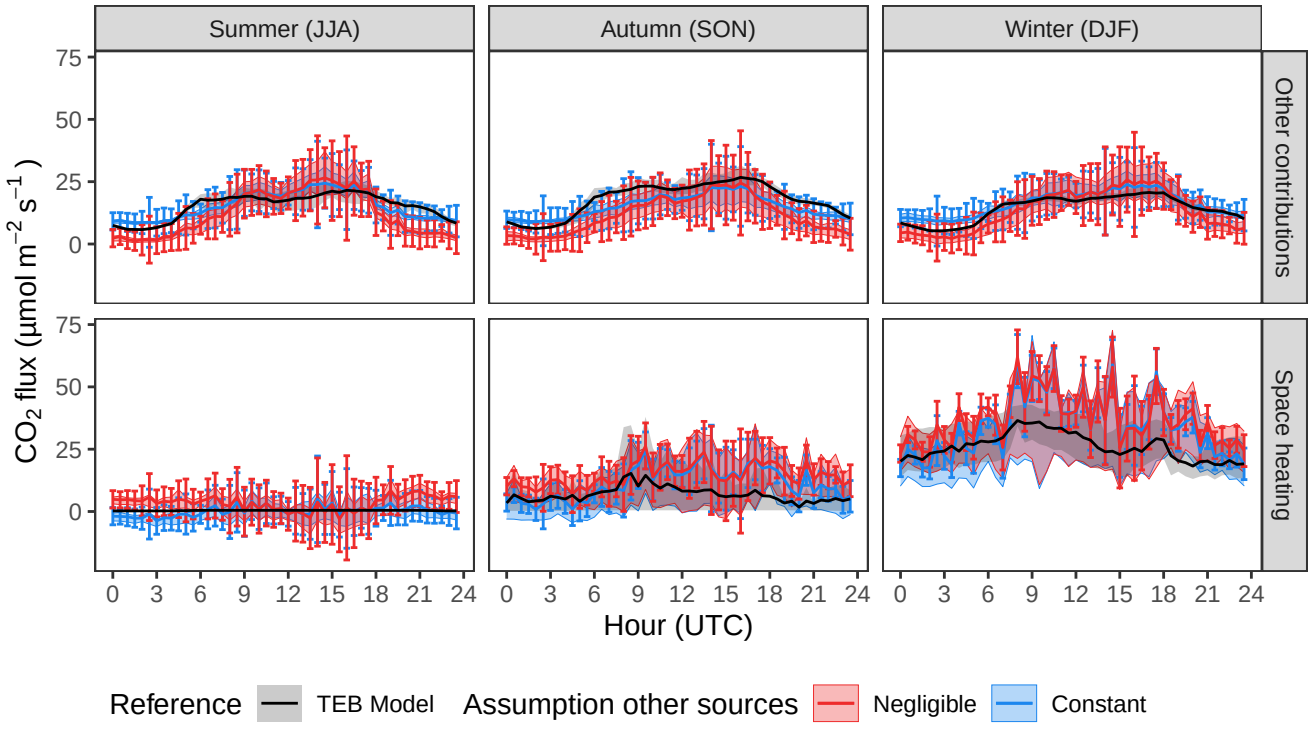

Figure 11: Mean daily cycles of CO_2 fluxes in the center of Toulouse. The contribution from space heating (bottom) is separated from the other contributions (top). The coloured areas represent the interquartile range. The error bars indicate the margin of uncertainty associated with the disaggregation method. The model data are those modelled by TEB with the REF configuration.